NASA/TM-20260000440

An Investigation Regarding the Effects of Volume Dynamics on Gas Turbine Engine Performance and Operability

Nolan M. LaMarche
HX5, LLC, Brook Park, Ohio

Thomas M. Lavelle and Jeffryes W. Chapman
Glenn Research Center, Cleveland, Ohio

January 2026

NASA STI Program Report Series

Since its founding, NASA has been dedicated to the advancement of aeronautics and space science. The NASA scientific and technical information (STI) program plays a key part in helping NASA maintain this important role.

The NASA STI program operates under the auspices of the Agency Chief Information Officer. It collects, organizes, provides for archiving, and disseminates NASA's STI. The NASA STI program provides access to the NTRS Registered and its public interface, the NASA Technical Reports Server, thus providing one of the largest collections of aeronautical and space science STI in the world. Results are published in both non-NASA channels and by NASA in the NASA STI Report Series, which includes the following report types:

- TECHNICAL PUBLICATION.
  Reports of completed research or a major significant phase of research that present the results of NASA programs and include extensive data or theoretical analysis. Includes compilations of significant scientific and technical data and information deemed to be of continuing reference value. NASA counterpart of peer-reviewed formal professional papers but has less stringent limitations on manuscript length and extent of graphic presentations.

- TECHNICAL MEMORANDUM.
  Scientific and technical findings that are preliminary or of specialized interest, e.g., quick release reports, working papers, and bibliographies that contain minimal annotation. Does not contain extensive analysis.

- CONTRACTOR REPORT.
  Scientific and technical findings by NASA-sponsored contractors and grantees.

- CONFERENCE PUBLICATION.
  Collected papers from scientific and technical conferences, symposia, seminars, or other meetings sponsored or cosponsored by NASA.

- SPECIAL PUBLICATION.
  Scientific, technical, or historical information from NASA programs, projects, and missions, often concerned with subjects having substantial public interest.

- TECHNICAL TRANSLATION.
  English-language translations of foreign scientific and technical material pertinent to NASA's mission.

Specialized services also include organizing and publishing research results, distributing specialized research announcements and feeds, providing information desk and personal search support, and enabling data exchange services.

For more information about the NASA STI program, see the following:

- Access the NASA STI program home page at http://www.sti.nasa.gov

NASA/TM-20260000440

An Investigation Regarding the Effects of Volume Dynamics on Gas Turbine Engine Performance and Operability

Nolan M. LaMarche
HX5, LLC, Brook Park, Ohio

Thomas M. Lavelle and Jeffryes W. Chapman
Glenn Research Center, Cleveland, Ohio

National Aeronautics and
Space Administration

Glenn Research Center
Cleveland, Ohio 44135

January 2026

Acknowledgments

This effort was funded by the Foundational Electrified Aircraft Propulsion subproject of NASA's Transformational Tools and Technologies project. The authors would like to thank Jonathan Kratz for his assistance in developing the optimized open-loop fuel flow schedule and electric machine torque profiles applied to the AGTF30 engine models as well as for supplying the turbomachinery flowpath dimensions from WATE++.

This work was sponsored by the
Transformative Aeronautics Concepts Program.

Level of Review: This material has been technically reviewed by technical management.

This report is available in electronic form at https://www.sti.nasa.gov/ and https://ntrs.nasa.gov/

NASA STI Program/Mail Stop 050
NASA Langley Research Center
Hampton, VA 23681-2199

An Investigation Regarding the Effects of Volume Dynamics on Gas Turbine Engine Performance and Operability

Nolan M. LaMarche
HX5, LLC
Brook Park, Ohio 44142

Thomas M. Lavelle and Jeffryes W. Chapman
National Aeronautics and Space Administration
Glenn Research Center
Cleveland, Ohio 44135

Abstract

This work explores the impact of adding volume dynamics to an electrified turbofan engine model. The zero-dimensional single-input single-output volume elements capture the physics of fluid compressibility of flow in the engine core gas path turbomachinery during transient operation with greater fidelity. Some background regarding the motivation for this effort is provided. A model of the volume element is developed from first principles. The baseline engine model is described and an explanation is given of the modifications made to incorporate the volume elements into the new model. Details of the simulated inputs, designed to elicit exaggerated dynamic responses and to facilitate comparison between the baseline and modified engine models, are explicated. The results of these simulations are presented and discussed, demonstrating that the transient performance and operability of the modified engine model, measured by parameters such as shaft speeds, thrust, and high-pressure compressor (HPC) stall margin, are impacted by the additional dynamics. Commentary is provided regarding potential explanations for the differences in behavior exhibited by the two models. Finally, suggestions are offered for future work that might improve the volume models developed in this effort and leverage the improved fidelity enabled by the modeling of turbomachinery volume dynamics.

Nomenclature

Acronyms

AGTF30	Advanced Geared Turbofan 30,000
BL	baseline model
COMB	combustor
FAR	fuel-to-air ratio
HP	high-pressure
HPC	high-pressure compressor
HPT	high-pressure turbine
LP	low-pressure
LPC	low-pressure compressor
LPT	low-pressure turbine
NPSS	Numerical Propulsion System Simulation
OL	operating line
SFC	specific fuel consumption
TEEM	Turbine Electrified Energy Management
T-MATS	Toolbox for the Modeling and Analysis of Thermodynamic Systems
VD	volume dynamics inclusive model
VLM	volume element
WATE++	Weight Analysis of Turbine Engine - an Object-Oriented Version

Variables

FAR	fuel-to-air ratio (-)
g	gravitational acceleration (in/s^2)
h	specific enthalpy (BTU/lb$_\mathrm{m}$)
h_t	specific total enthalpy (BTU/lb$_\mathrm{m}$)
M	mass (lb$_\mathrm{m}$)
N_2	low-pressure shaft speed (RPM)
N_3	high-pressure shaft speed (RPM)
t	time (s)
$\dot{Q}_{cv}$	rate of external heat transfer to fluid within control volume (BTU/s)
U	internal energy (BTU)
u	specific internal energy (BTU/lb$_\mathrm{m}$)
V	volume (in^3)
W	mass flow rate (lb$_\mathrm{m}$/s)
$\dot{W}_{cv}$	rate of work performed by fluid within control volume (BTU/s)
z	vertical distance from datum (in)
ρ	density (lb$_\mathrm{m}$/in^3)

1 Introduction

Gas turbine engines constitute the means of propulsion for the preponderance of global air traffic (Ref. 1). As such, NASA has historically played a role in advancing the state of the art of this technology, conducting research which, among other outcomes, has led to increased efficiency and thus reduced expenditures for both civilian and military aircraft operators.

Electrified (sometimes referred to as *more electric*) propulsion solutions have been the subject of increased interest in recent years among industrial, academic, and governmental stakeholders as a novel method by which gas turbine engine efficiency can be improved. NASA, through its commercial partnerships and fundamental research, has maintained a role in the study of such systems and the technology development efforts required to make them feasible for adoption into commercial operation. While many electrified propulsion architectures have been proposed (Ref. 1), the hybrid electric and turboelectric variants — those of interest to NASA as a result of their candidacy for application to the aircraft classes accounting for the majority of air traffic — share the common feature of employing electric machines (also known as motor/generators) to augment the capabilities of traditional gas turbine engines.

Aircraft engine cycle models, particularly those used for controls development, have historically tended to focus on engine shaft speed dynamics while ignoring faster dynamics that are more difficult to accurately model and measure. A typical approach, as in the Numerical Propulsion System Simulation (NPSS) (Ref. 2), is for engine components to be represented as discrete lumped elements throughout which mass flow rate is conserved at every time step in a dynamic simulation. The transient behavior of the engine is captured by calculating the net torques acting upon the engine shafts at each time step and employing simple dynamic equations representing the inertial reaction of the shafts to determine their angular accelerations. These are then integrated to obtain the shaft speeds in the subsequent time step, and the process is repeated. While this approach has been generally sufficient for capturing the dynamics of the engine shaft, which dominate the response of the system, it does not account for the more granular effects in the gas path (Ref. 3). An augmented modeling approach is required for greater fidelity.

Volume dynamics refers to the effects exhibited by the air in the engine gas path during transient operation. The term *volume packing* is also used in the literature to refer to this phenomena (Ref. 4). As the engine throttle is adjusted, more or less fuel will be supplied to the combustor, manifesting in a change in the mass flow rate, energy, and fuel-to-air ratio (FAR) in the downstream flow. This, in turn, will result in a change in the net torque contributions to the engine spools from the turbine blades, causing the shaft speeds to adjust accordingly, inducing further changes in engine flow properties. However, this process results in a momentary mismatch between the up- and downstream flow conditions across each element. Accounting for volume dynamics in engine models allows for simulations to capture these unsteady flow effects.

This behavior has historically been deemed too subtle to merit inclusion in air-breathing thermodynamic cycle models. Legacy effectors and actuators respond with time constants on the order of 10s of milliseconds, far too long to enact any meaningful response to gas path dynamics before their effects dissipate. However, the electric machines included as part of electrified propulsion schemes offer greatly increased bandwidth for both sensing and actuation. Higher-fidelity modeling approaches offer greater insights into more subtle engine behaviors, potentially enabling improvements to engine performance and operability via novel control strategies that leverage electrified engine configurations.

2 Modeling and Simulation

This investigation seeks to explore how the behavior of an aircraft propulsion cycle model is affected by the inclusion of volume dynamics in the governing equations of the system. In subsection 2.1, the physics of the volume element to be implemented in an engine system model are developed. In subsection 2.2, an overview is provided of the baseline engine model into which the volume components will be incorporated. In subsection 2.3, a description is given regarding the approach taken toward exercising the baseline and modified engine models in simulation with the expectation that any differences between the two will be attributable to the inclusion of the volume elements in the modified engine model.

2.1 Volume Element Model

To test the effects of volume dynamics in an engine model, a generalized volume element that accurately represents the physics of interest — at least, at the level of granularity required for controls development — must first be developed. Such volume elements (the term *plenum* is also frequently employed in the literature (Ref. 5)) are implemented in a variety of formats. However, they are always formulated such that they may be integrated within the target engine model. In the case at hand, NASA's subsonic air-breathing propulsion controls models are predominantly constructed using the internally developed Toolbox for the Modeling and Analysis of Thermodynamic Systems (T-MATS) (Ref. 6), a Simulink® blockset available for public download.

T-MATS consists of a collection of elements that represent the components of a gas turbine engine. The elements contain the relevant thermodynamic and fluid physics of the zero-dimensional component representation and can be linked together to compose a propulsion system cycle model. T-MATS takes a quasi-steady approach to transient simulation, i.e., at a given time step, the thermodynamic relations expressed in the system components operate no differently during a transient than during steady state operation. The steady state solution is used to calculate the angular accelerations of the engine shafts, but these expressions alone do not provide the full picture of the engine's behavior during transient operation. An aim of this effort is to augment this quasi-steady modeling approach through the inclusion of volume dynamics.

Rather than develop an entire new set of component models that account for the volume dynamics in each respective element (Ref. 7), a simpler, though perhaps lower fidelity, approach is to employ these volume elements in series with the turbomachinery component models. Thus, each component model is coupled with an associated volume that incorporates the flow rate, energy, and composition dynamics prescribed in the volume model.

As such, a zero-dimensional volume element is developed in alignment with the schematic in Figure 1. The incoming and outgoing flows each exhibit some mass flow rate, specific total enthalpy, and FAR. At steady state, there should be no imbalance in any of these physical quantities across the volume element. The volume dynamics are expressed through a system of differential equations representing the conservation of mass, conservation of energy, and conservation of composition in Equation 1, Equation 2, and Equation 3, respectively. This approach leverages a formulation that has historically been applied to rocket engine modeling in which the effects of volume dynamics are of significantly greater concern. Details on the development of the governing dynamic equations implemented in the volume element are provided in the Appendix.

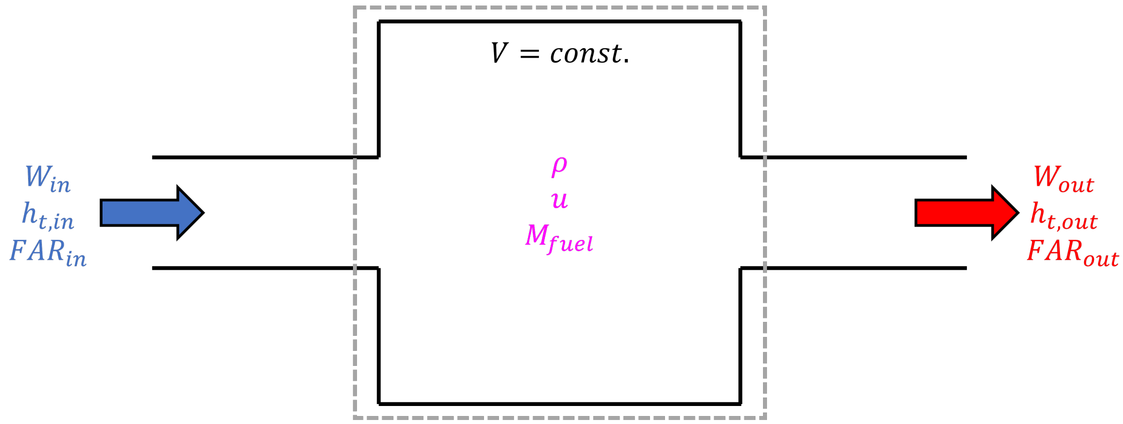

Figure 1.—Depiction of the zero-dimensional volume element model with inflow and outflow state variables and internal fluid characteristics denoted

$$\dot{\rho} = \frac{W_{in} - W_{out}}{V} \tag{1}$$

$$\dot{u} = \frac{W_{in}h_{t,in} - W_{out}h_{t,out} - u(W_{in} - W_{out})}{\rho V} \tag{2}$$

$$\dot{M}_{fuel} = W_{in}\left(\frac{FAR_{in}}{1 + FAR_{in}}\right) - W_{out}\left(\frac{FAR_{out}}{1 + FAR_{out}}\right) \tag{3}$$

2.2 Engine Model

The volume element developed in subsection 2.1 must be incorporated into a larger system model to investigate the effects of volume dynamics on a gas turbine engine. The Advanced Geared Turbofan 30,000 (AGTF30) (Ref. 8), an engine model developed at the NASA Glenn Research Center, is used for the present study. Constructed of elements from the T-MATS blockset, the AGTF30 is based on the conceptual N+3 engine (Ref. 9) developed as a benchmark model for a geared turbofan with a projected entry-into-service date some time in the early 2030s. The AGTF30 model has been used in numerous controls development studies both by NASA as well as its external partners in industry and academia and is available online for public download.

The AGTF30 model was modified for the present study to exhibit volume dynamics in addition to the standard shaft speed dynamics included in the baseline model. This was accomplished by introducing a volume element block downstream of each turbomachinery component of the AGTF30 core, namely, the low-pressure compressor (LPC), high-pressure compressor (HPC), high-pressure turbine (HPT), and low-pressure turbine (LPT). Figure 2 provides a block diagram depiction of the components and connections within the modified AGTF30 model core. The introduction of the volume elements permits the incoming and outgoing flows to exhibit varying mass flow rates, enthalpies, and FARs during transient operation. Any imbalance in these quantities will result in a change to the dynamic state variables (density, specific internal energy, and fuel mass) defined for the fluid within each volume.

Turbomachinery component dimensions were obtained using the NASA–Boeing developed Weight Analysis of Turbine Engine - an Object-Oriented Version (WATE++) code (Ref. 10). This program estimates the physical dimensions of an engine based on its propulsion cycle model.

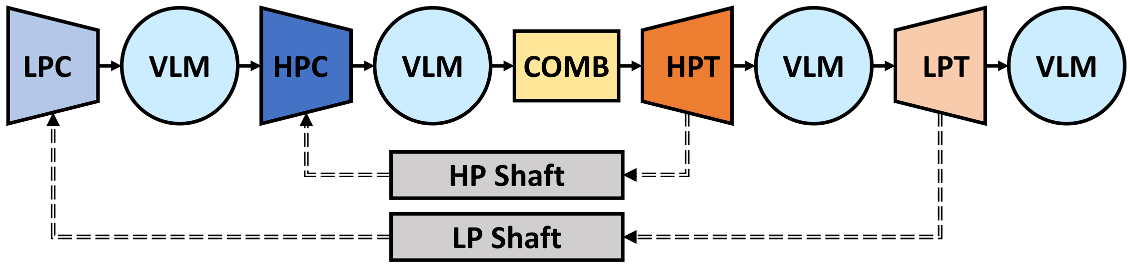

Figure 2.—Notional representation of the component-level model of the AGTF30 engine core with the newly-introduced volume elements depicted; note that bleeds and ducts are ignored in the diagram for simplicity

In this case, the model of NASA's notional N+3 engine was used because it served as the basis for the T-MATS model of the AGTF30. The graphical output from the WATE++ code can be seen in Figure 3 while the turbomachinery component volumes — calculated using the flow area and stage lengths output by the WATE++ code — are shown in Table 1.

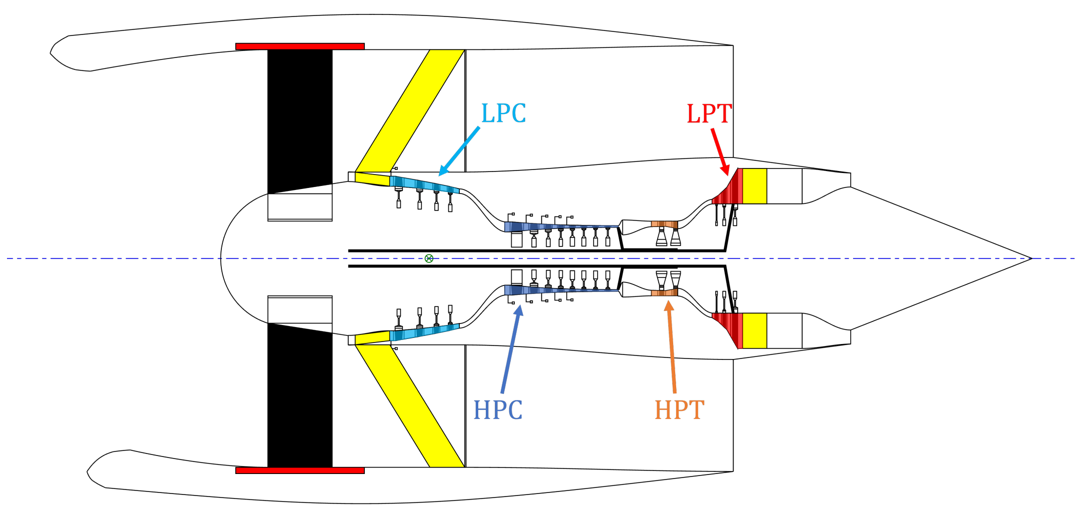

Figure 3.—Graphical depiction of the N+3 engine cross-section from WATE++ with core turbomachinery components highlighted

Table 1.—Core turbomachinery component flowpath volumes for the N+3 engine from WATE++ (calculated as a summation of the products of stage flow areas and lengths)

Component	Volume (in^3)
LPC	2081
HPC	1259
HPT	208
LPT	1257

2.3 Simulation Inputs

To exercise the model described in subsection 2.2, simulation test cases were formulated to excite the dynamics of the volume elements. The same inputs to the new model were provided to the unmodified AGTF30 model, creating a baseline for comparison. Any differences in the response of the modified model relative to that of the baseline are thus attributable to the introduction of the volume elements into the engine core of the model under study.

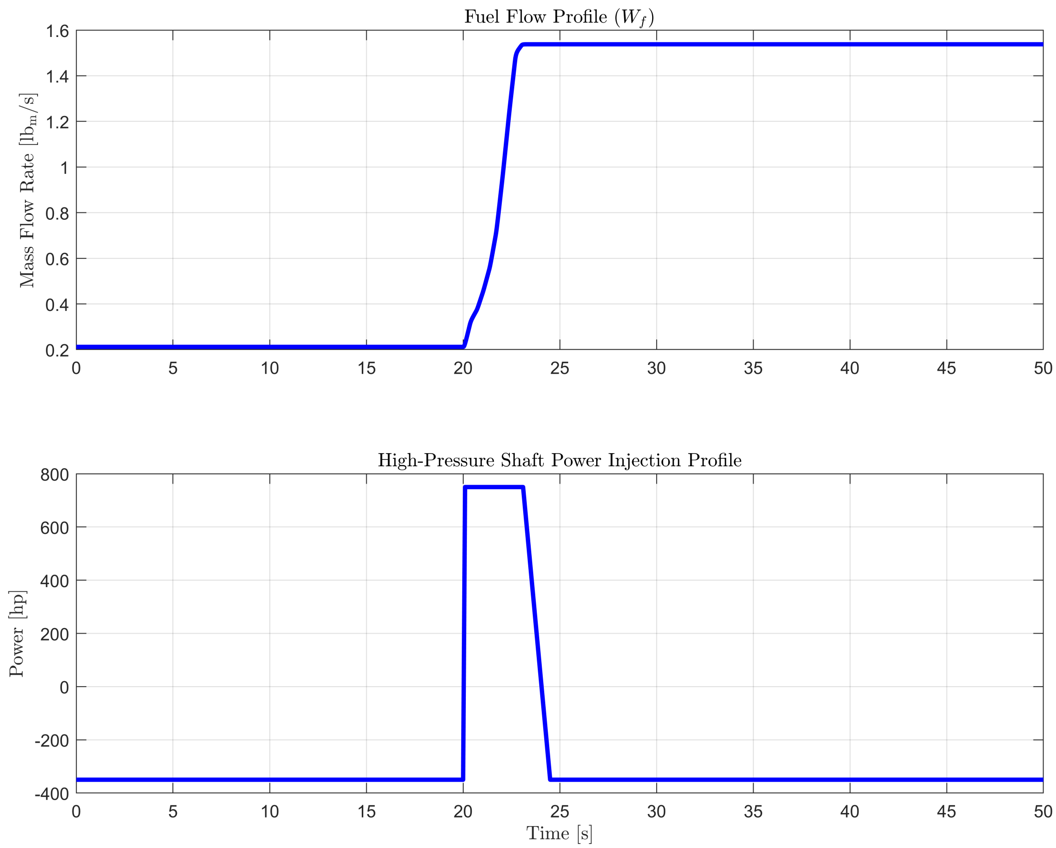

Figure 4.—Fuel flow rate and power injection profiles applied to the baseline and volume dynamics inclusive AGTF30 models; Note: A constant power extraction of 350 hp is applied to the high-pressure (HP) shaft under steady state conditions to account for airframe electrical loads, so a positive increase relative to this nominal value represents power *injection* to the shaft.

To elicit a more exaggerated response than is achievable when the limiters in the engine control logic are active, the model was supplied with an open-loop takeoff fuel flow profile, which compressed the typical idle-to-maximum thrust request timeline from 5 to 3 seconds. Additionally, the HP shaft was supplied with a power injection profile during this transient period to emulate the effects of the Turbine Electrified Energy Management (TEEM) control approach (Ref. 11). In short, TEEM aims to mitigate the off-nominal behavior exhibited by the turbomachinery components during transient operation by strategically injecting or extracting power via an electric machine to one or both shafts, depending on the electrified architecture and transient scenario. While such system-level considerations are outside the scope of this effort, different propulsion architectures might draw energy from a battery, a fuel cell, or another engine shaft to enable power injection. The present study focused on injection to the HP spool due to the nature of the HPC as the component most likely to enter stall during acceleration. The manual fuel flow and power injection profiles supplied to both engine models are depicted in Figure 4. Note that the AGTF30 model includes a constant power debit term of 350 hp to account for the electrical draw from auxiliary aircraft systems. One may observe that this is represented by a constant negative value before and after the transient in Figure 4. Thus, any *positive* increase from this baseline represents the quantity of power injected at a given instant.

T-MATS allows the system to be solved using the Newton-Raphson method to iteratively adjust several independent parameters (one for each turbomachinery component and nozzle), driving their associated residual errors to zero. The reduction of these error terms, or *dependents*, ensures that mass conservation is satisfied across the individual engine components. The incorporation of the volume blocks into the flow path introduces discontinuities in flow state variables throughout the engine, allowing for the dynamics described by the differential equations in subsection 2.1 to be captured. However, each volume element includes three additional independents, each with three dependents that must be minimized by the Newton-Raphson solver to reach a solution. With the addition of four volume elements, the Jacobian for the modified engine system grows from a 7x7 matrix to a 19x19 matrix, greatly increasing the required computational effort for the solver to achieve convergence at each time step. Through trial-and-error, the apparent largest dynamic time step for which the standard Newton-Raphson solver could reliably achieve convergence of the modified model was found to be 30 μs, smaller than the standard 15 ms time step by a factor of 500. As such, this time step size was specified for the simulation of both engine models. While the results from the baseline model at the 30 μs time step are virtually identical to those obtained at a step size of 15 ms, using the same time step for both simulations enabled a direct point-by-point comparison of the two responses.

3 Results

As discussed, simulation of the AGTF30 with volume dynamics within the existing T-MATS framework required some adjustments to the standard solver configuration which resulted in significantly increased computational times relative to standard runs of the unmodified AGTF30. A typical execution of the simulations presented here on a workstation equipped with an 11th Gen Intel Core i7-11850H processor (2.50 GHz) and 32 GB of RAM required approximately 645 seconds for the baseline and 818 seconds for the volume dynamics case, respectively. The exceedingly small time step required to conduct this study suggests that volume dynamics inclusive models are less suitable for implementation in real-time simulations and in system studies where large numbers of simulations are required to explore the trade space. The additional elements add complexity to the model, increasing the computational intensity needed to reach convergence at each time step. Additionally, the smaller time step necessitates that the computation required to simulate the engine cycle and achieve convergence of the solver's dependent parameters be completed for a significantly greater number of iterations, severely inhibiting real-time implementation. More advanced solvers than the standard Newton-Raphson method used in this study may reduce these barriers through a combination of greater robustness to dependent sensitivity and computational efficiency.

To compare the responses of the two engine models, one may observe the low- and high-pressure engine core shaft speeds (N_2 and N_3, respectively) throughout the simulation since these are the dynamic elements present in both systems. It can be seen from Figure 5 that the shaft speeds of the modified AGTF30 (VD) roughly track those of the baseline model (BL) throughout the transient, though VD consistently lags BL. The two models demonstrate agreement before and after the transient, confirming that the additional volume elements in the modified engine model do not impact its steady state operation. However, as soon as the fuel flow rate is increased, the modified AGTF30 model exhibits an increase in both shaft speeds, albeit with VD increasingly lagging BL. This variance increases until the fuel flow rate reaches its new steady state condition around 23 seconds, at which point the relative difference in the two shaft speeds diminishes within about 2 seconds as the apparent lag dissipates. This demonstrates that, as expected, any change in the behavior of the volume dynamics inclusive AGTF30 model will manifest in a modified dynamic response, which occurs during transient operation.

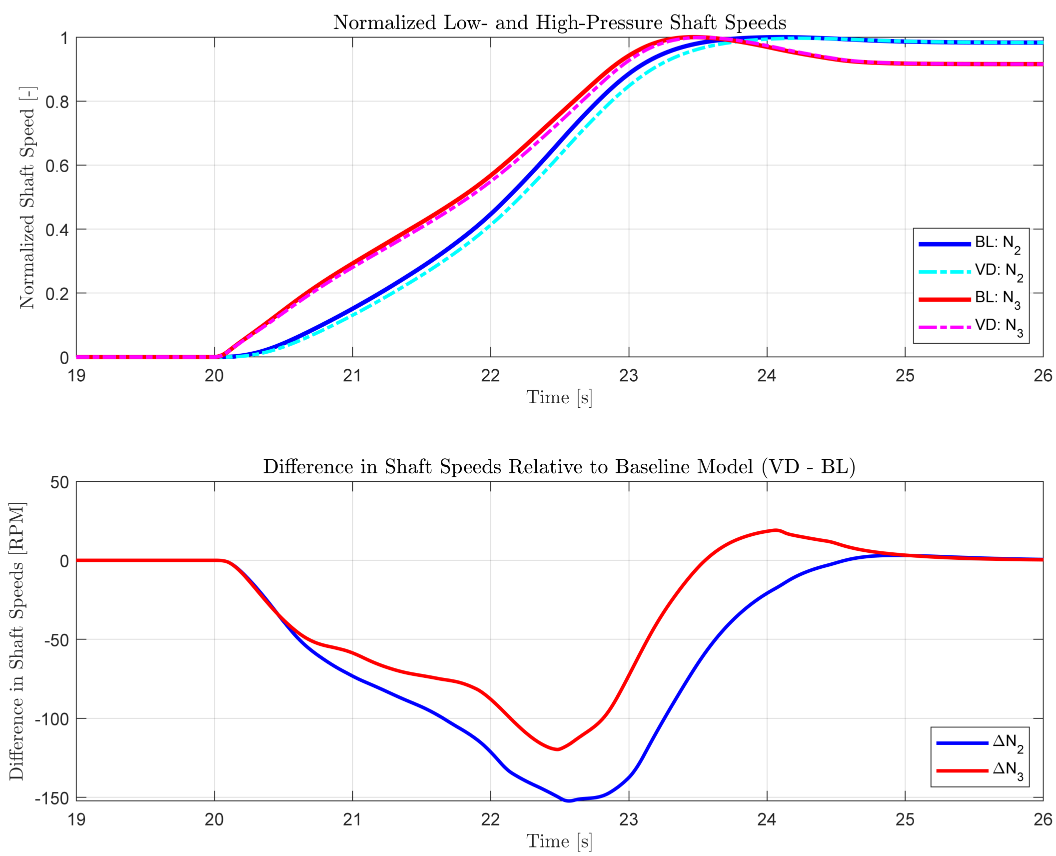

Figure 5.—Comparison of baseline and modified AGTF30 engine model shaft speeds subject to a manual idle-to-max thrust fuel flow profile with HP shaft power injection; Shaft speeds normalized by their maximum and minimum transient values; Note that VD lags BL during the transient

The transient dependence of this behavior is most evident upon examination of the dynamic variables of each volume element: density, specific internal energy, and fuel mass accumulation. Figure 6 displays the state variables and their derivatives for each volume element in the core stream of the modified AGTF30 model during the period in which fuel flow is increasing and additional power is being supplied to the HP shaft. One may observe that the variables all begin to exhibit dynamic behavior only upon actuation of the fuel flow rate and power injection and that the rate-of-change variables begin a transition back to zero as these inputs stabilize at their final values. Note that, due to their physical locations upstream of the combustor, the LPC and HPC volume elements do not exhibit any dynamic behavior regarding accumulated fuel mass. Also note that the rate-of-change variables, particularly $\dot{u}_t$ and $\dot{M}_{fuel}$, exhibit a high degree of numerical noise. This behavior is likely a result of the sensitivity of these variables to changes in the independent parameters used in the T-MATS Newton-Raphson solver to achieve convergence. To enable convergence in the dynamic simulation, numerical tolerances for the modified engine model were relaxed by an order of magnitude. This yields increased numerical noise, though much of it is filtered out of the state variables by the integration process as exhibited in Figure 6.

Two variables of interest regarding the performance of an air-breathing propulsion engine are the thrust it produces and its specific fuel consumption (SFC), a measure of the fuel consumption of the engine relative to the thrust it generates. Figure 7 provides a comparison of these two parameters across the baseline and modified AGTF30 models. As in the case of the shaft speeds, the thrust produced by the volume dynamics inclusive engine model appears to lag the baseline engine model. However, any difference in thrust between the two models is increasingly marginal after the fuel flow profile reaches its maximum around 23 seconds, with the deviation between the models reducing to an effectively negligible amount around 24 seconds. This decreased thrust manifests in a consistently higher SFC in the modified engine model throughout the transient period. One potential explanation for this difference in behavior is that the lower-fidelity baseline model does not accurately predict the dynamics of the mass flow rates through the engine core. The modified mass flow rate dynamics result in a lag in thrust response and thus in SFC as well.

One major contributing factor to the increased transient SFC can be seen through examination of the transient trajectories of each engine model's operating points on the HPC map as depicted in Figure 8. During a normal increasing throttle transient in which no power is injected to the HP shaft, the acceleration operating point trajectory will exhibit a positive excursion away from the steady state operating line — i.e., movement toward the stall line. This off-design excursion results in a reduction of the available stability (or stall) margin in the component. Emulating TEEM, power injection during the transient serves to collapse this trajectory closer to operating line, resulting in a greater stability margin and, generally, higher component efficiency during the transient period. This closer adherence to on-design behavior is exhibited in the baseline case, as seen in Figure 8. However, the volume dynamics case appears to exhibit a *negative*-excursion trajectory during the transient, resulting in improved off-design operability from the baseline. Looking to Figure 9, one may observe that this negative excursion manifests in a consistently *greater* stall margin during the transient than is seen in the baseline case. Given that without TEEM, an *increasing* throttle transient results in a *positive* transient excursion from the operating line, the *negative* excursion demonstrated in the volume dynamics case in Figure 8 would seem to imply that the reduced stall margin exhibited in Figure 9 is a result of greater power injection on the HP shaft than is necessary to collapse the HPC operating point transient trajectory along the steady state operating line. The results obtained in this study

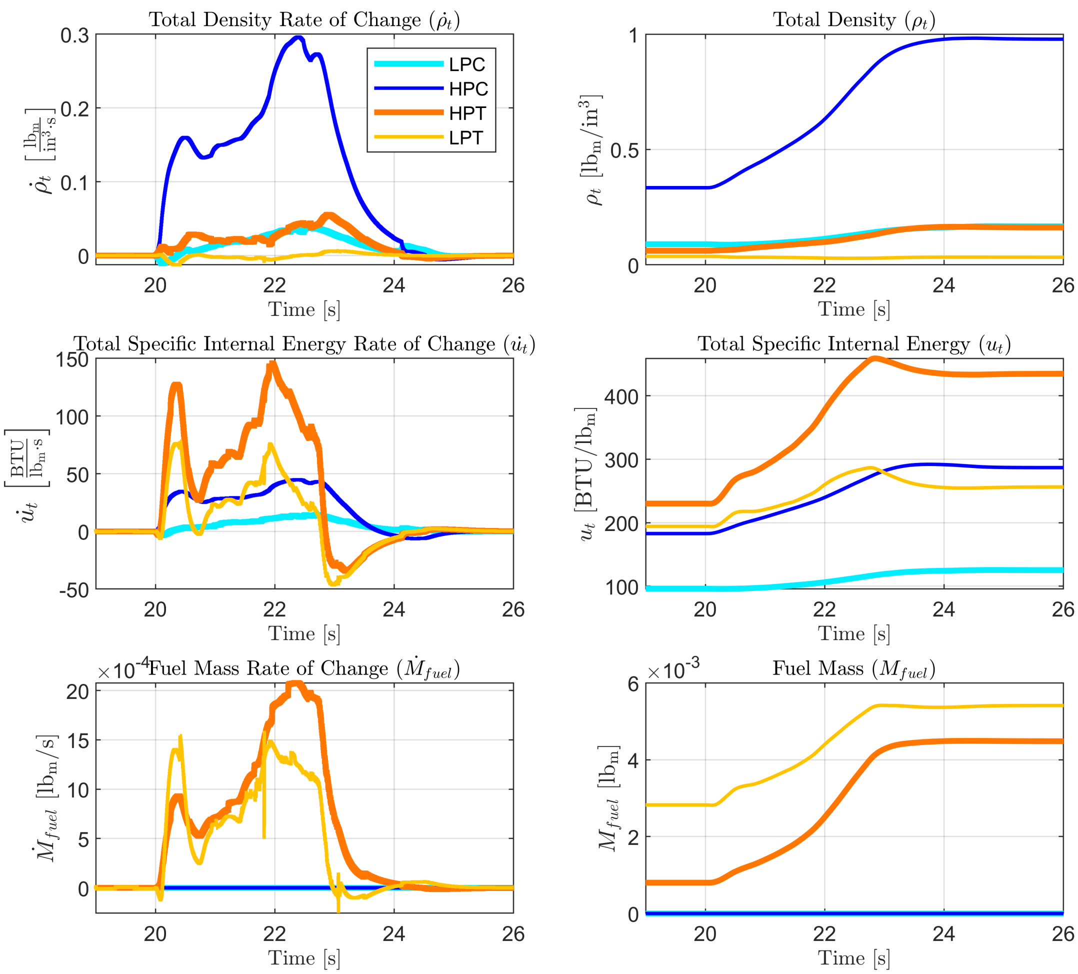

Figure 6.—Dynamic state variables and their derivatives from each volume element corresponding to a turbomachinery component in the AGTF30 core stream

imply that optimal HPC efficiency in the modified AGTF30 might be maintained with less external power applied to the HP shaft. Assuming the volume dynamics inclusive model more accurately represents a true engine response, this indicates that the benefits of TEEM are achievable with less energy expenditure than estimated with the baseline model. However, a fair comparison of the TEEM impact will achieve the same thrust response time, and it is acknowledged that while the volume dynamics model exhibits improved operability, it also has a slower thrust response.

4 Conclusion

The present study investigated the effects of volume dynamics on gas turbine engine behavior through the development of a dynamic volume element model, the incorporation of several such

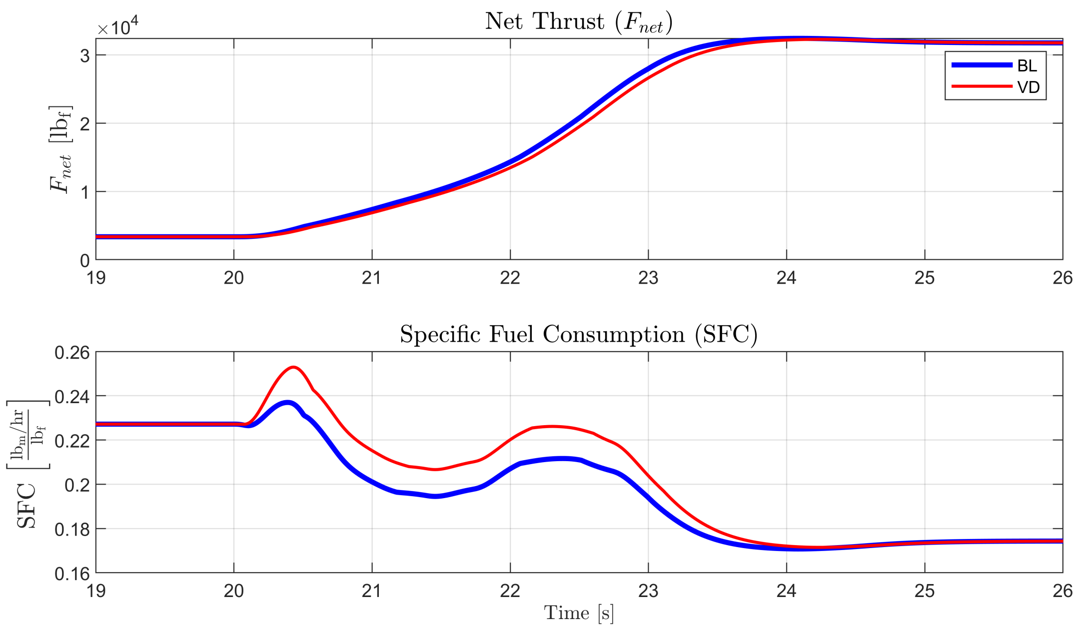

Figure 7.—Comparison of the net thrust and specific fuel consumption exhibited by the baseline and modified AGTF30 models during the idle-to-max power transient period

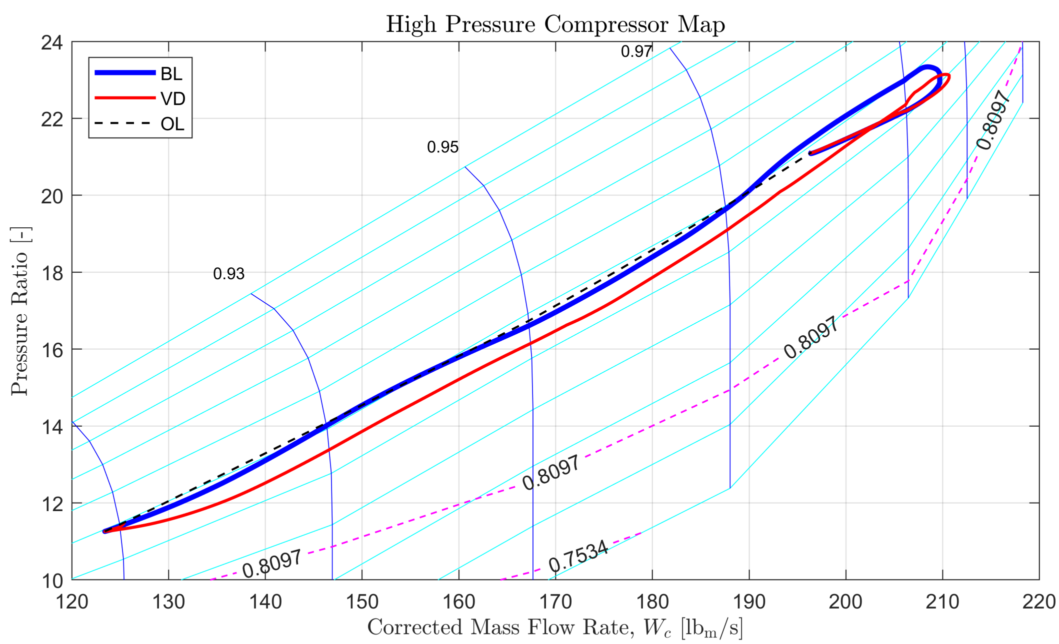

Figure 8.—Transient operating point trajectories for the baseline and volume dynamics inclusive AGTF30 overlaid with the steady state operating line on the HPC map

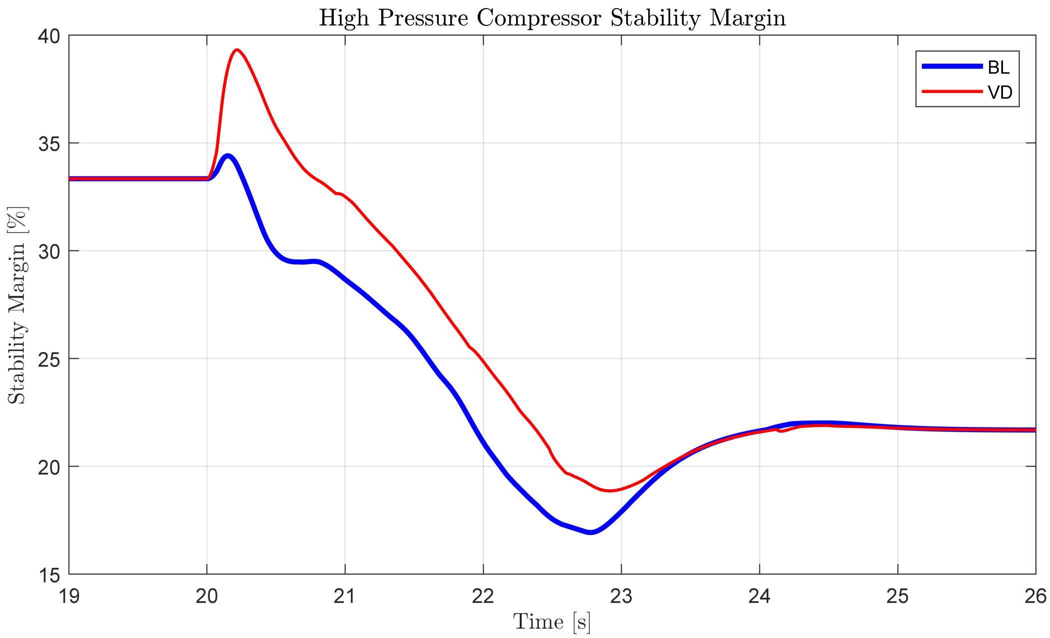

Figure 9.—High-pressure compressor stall margin for both the baseline and volume dynamics inclusive AGTF30 models during the transient period

elements into the core stream of an air-breathing propulsion cycle model, and the simulation of this model during an engine acceleration when subject to an increasing fuel flow rate and power injection to its HP shaft. The resulting behavior of this new model was compared to the unmodified engine model without the new volume elements, serving as a baseline for isolating the effects of the newly introduced dynamics to the overall system response. Examination of the simulated model outputs demonstrated varying responses resulting from the additional dynamics in the modified model. In the modified model, thrust was consistently lower while SFC was consistently higher during the transient period. The transient operating point trajectories charted on the HPC map, taken together with the modeled stability margins, imply that less power injection is required to reduce transient excursion from the operating line than is predicted when only shaft dynamics are accounted for. The results suggest that control design and electric machine sizing for TEEM concepts performed with only shaft dynamics inclusive models will provide a good basis for such an architecture, but that consideration of volume dynamics could impact electrical system requirements and enable further benefits.

There are many potential avenues for furthering the modeling and simulation approaches developed in this effort. The physics implemented in the volume elements may be augmented by accounting for the conservation of momentum as other authors have explored (Ref. 12). While such additional fidelity was neglected in this work, future studies may reveal results that vary from those obtained here. Such granularity should provide greater insight into the dynamic response of the engine when subject to transient phenomena and might be used to inform improved control strategies for maintaining optimal transient performance. Investigations into different fuel flow profiles, throttle maneuvers, and power augmentation strategies may yield insights into how to best leverage the improved fidelity afforded by volume dynamics inclusive modeling in simulations of gas turbine engines. In addition, among the extensive range of potential architectures and configurations of future gas turbine engine systems, including electrified systems and advanced cycles, there are numerous benefits, challenges, and control capabilities that can be leveraged for operational optimization. The volume dynamics modeling tools developed through this effort and described herein provide a means for more accurately assessing transient concerns of such systems without immediately necessitating computationally intensive high-fidelity modeling methods such as computational fluid dynamics. In contrast to such methods, the approach developed here is more amenable for inclusion within models for control testing and evaluation.

References

1. National Academies of Sciences, Engineering, and Medicine: *Commercial Aircraft Propulsion and Energy Systems Research: Reducing Global Carbon Emissions*. The National Academies Press, Washington, DC, 2016. URL `https://nap.nationalacademies.org/catalog/23490/commercial-aircraft-propulsion-and-energy-systems-research-reducing-global-carbon`.

2. Lytle, J. K.: The Numerical Propulsion System Simulation: An Overview. NASA Technical Memorandum NASA/TM-2000-209915, NASA, 2000. URL `https://ntrs.nasa.gov/citations/20000063377`.

3. Kurzke, J.; and Halliwell, I.: *Propulsion and Power: An Exploration of Gas Turbine Performance Modeling*. Springer, Cham, Switzerland, 2018.

4. DeSmidt, H. A.; Smith, E. C.; Bill, R. C.; and Wang, K.-W.: Comprehensive Modeling and Analysis of Rotorcraft Variable Speed Propulsion System With Coupled Engine/Transmission/Rotor Dynamics. NASA Contractor Report NASA CR-2013-216502, NASA, 2013. URL `https://ntrs.nasa.gov/citations/20130014755`.

5. Camporeale, S.; Fortunato, B.; and Mastrovito, M.: A Modular Code for Real Time Dynamic Simulation of Gas Turbines in Simulink. *Journal of Engineering for Gas Turbines and Power*, vol. 128, 07 2006, pp. 506–517.

6. Litt, J. S.: Toolbox for the Modeling and Analysis of Thermodynamic Systems (T-MATS) Users' Workshop Presentations. NASA Conference Publication NASA/CP—2018-219785, NASA, 2018. URL `https://ntrs.nasa.gov/citations/20180002976`.

7. Kopasakis, G.; Connolly, J. W.; Paxson, D. E.; and Ma, P.: Volume Dynamics Propulsion System Modeling for Supersonics Vehicle Research. *Journal of Turbomachinery*, vol. 132, 10 2010, p. 041003.

8. Chapman, J. W.; and Litt, J. S.: Control Design for an Advanced Geared Turbofan Engine. NASA Technical Memorandum NASA/TM—2017-219569, NASA, 2017. URL `https://ntrs.nasa.gov/citations/20170011210`.

9. Jones, S. M.; Haller, W. J.; and Tong, M. T.-H.: An N+3 Technology Level Reference Propulsion System. NASA Technical Memorandum NASA/TM-2017-219501, NASA, 2017. URL `https://ntrs.nasa.gov/citations/20170005426`.

10. Tong, M. T.; and Naylor, B. A.: An Object-Oriented Computer Code for Aircraft Engine Weight Estimation. ASME, vol. Volume 1: Aircraft Engine; Ceramics; Coal, Biomass and Alternative Fuels; Manufacturing, Materials and Metallurgy; Microturbines and Small Turbomachinery of *Turbo Expo*, 06 2008, pp. 1–7. URL `https://doi.org/10.1115/GT2008-50062`.

11. Culley, D. E.; Kratz, J. L.; and Thomas, G. L.: Turbine Electrified Energy Management (TEEM) For Enabling More Efficient Engine Designs. Joint Propulsion Conference, AIAA, 07 2018. URL `https://arc.aiaa.org/doi/abs/10.2514/6.2018-4798`.

12. Argote, C.; Kestner, B. K.; and Mavris, D. N.: NPSS Volume Dynamic Capability for Real-Time Physics Based Engine Modeling. ASME, vol. Volume 1: Aircraft Engine; Ceramics; Coal, Biomass and Alternative Fuels; Wind Turbine Technology of *Turbo Expo*, 06 2011, pp. 139–148. URL `https://doi.org/10.1115/GT2011-45374`.

5 Appendix

In the analysis below, performed to obtain the governing dynamic equations for the volume element used in this study, the following assumptions are made:

- No external heat is exchanged across the control volume boundary of the element.
- No work is performed on the fluid by the volume, and vice versa.
- There is no change in the pressure of the flow across the volume.
- The flows into and out of the element, as well as the characteristics of the fluid within the element, are unsteady. Thus, all fluid parameters are subject to vary with time.
- The volume of the component is constant regardless of changes to the fluid within the element.

The dynamic equation for density, expressing the conservation of mass within the volume element depicted in Figure 1, is obtained as follows: A mass rate balance will be applied to obtain the time rate of change of mass within the volume, expressed as the difference between the mass flow rates into and out of the volume at a given instant in time:

$$\frac{dM}{dt} = W_{in} - W_{out} \tag{4}$$

Substituting for the definition of mass as a function of density and volume ($M = \rho V$):

$$\frac{d(\rho V)}{dt} = W_{in} - W_{out} \tag{5}$$

Leveraging the constant volume assumption and rearranging:

$$\boxed{\dot{\rho} = \frac{W_{in} - W_{out}}{V}} \tag{6}$$

The dynamic equation for the specific internal energy within the volume element is obtained by applying the conservation of energy. Here, the energy rate balance expresses the time rate of change of internal energy within the volume as the sum of the rates of heat transfer, work, and flow energy into and out of the volume at a given instant in time:

$$\frac{dU}{dt} = \dot{Q}_{cv} - \dot{W}_{cv} + W_{in}\left(h_{in} + \frac{V_{in}^2}{2} + gz_{in}\right) - W_{out}\left(h_{out} + \frac{V_{out}^2}{2} + gz_{out})\right) \tag{7}$$

Substituting for $U = Mu$ (where M and u are both variable with time), leveraging the assumptions that there is no external heat transfer across the control volume ($\dot{Q}_{cv} = 0$) and that no work is performed on or by the fluid ($\dot{W}_{cv} = 0$), and applying the definition of total enthalpy, $h_t = h + \frac{V^2}{2}$:

$$\frac{d(Mu)}{dt} = \dot{Q}_{cv} - \dot{W}_{cv} + W_{in}\left(h_{t,in} + gz_{in}\right) - W_{out}\left(h_{t,out} + gz_{out})\right) \tag{8}$$

Applying the product rule to the left-hand side, evaluating the right-hand side, and rearranging:

$$M\dot{u} + u\dot{M} = W_{in}h_{t,in} - W_{out}h_{t,out} + W_{in}gz_{in} - W_{out}gz_{out} \tag{9}$$

Using $z_{in} = z_{out}$ (since all turbomachinery components revolve around the same central axis), substituting for $M = \rho V$, and rearranging:

$$\rho V\dot{u} = W_{in}h_{t,in} - W_{out}h_{t,out} + gz(W_{in} - W_{out}) - u\dot{M} \tag{10}$$

Letting z = 0, substituting for the definition of $\dot{M}$ from Equation 4, and rearranging:

$$\boxed{\dot{u} = \frac{W_{in}h_{t,in} - W_{out}h_{t,out} - u(W_{in} - W_{out})}{\rho V}} \tag{11}$$

As a corollary to the conservation of mass, the volume element also obeys a conservation of composition. That is, the mass of fuel within the component is conserved. A modified form of the mass rate balance is applied, expressing the time derivative of the mass of fuel within the volume:

$$\frac{dM_{fuel}}{dt} = W_{fuel,in} - W_{fuel,out} \tag{12}$$

Multiplying the numerator and denominator of each term on the right-hand side by the definition of mass flow rate in the gas path as the sum of the air and fuel mass flow rates: $W = W_{air} + W_{fuel}$

$$\dot{M}_{fuel} = \frac{(W_{air,in} + W_{fuel,in})W_{fuel,in}}{W_{air,in} + W_{fuel,in}} - \frac{(W_{air,out} + W_{fuel,out})W_{fuel,out}}{W_{air,out} + W_{fuel,out}} \tag{13}$$

Dividing the numerator and denominator of each term on the right-hand side by W_{air} :

$$\dot{M}_{fuel} = \frac{(W_{air,in} + W_{fuel,in})\frac{W_{fuel,in}}{W_{air,in}}}{1 + \frac{W_{fuel,in}}{W_{air,in}}} - \frac{(W_{air,out} + W_{fuel,out})\frac{W_{fuel,out}}{W_{air,out}}}{1 + \frac{W_{fuel,out}}{W_{air,out}}} \tag{14}$$

Using the definitions $W = W_{air} + W_{fuel}$ and $FAR = W_{fuel}/W_{air}$:

$$\boxed{\dot{M}_{fuel} = W_{in}\left(\frac{FAR_{in}}{1 + FAR_{in}}\right) - W_{out}\left(\frac{FAR_{out}}{1 + FAR_{out}}\right)} \tag{15}$$